applied sciences

MDPI

Article

Resonant X-ray Emission Spectroscopy with a SASE Beam

Wojciech Błachucki [1,*], Yves Kayser [2], Anna Wach [1], Rafał Fanselow [1], Christopher Milne [3], Jacinto Sá [4] and Jakub Szlachetko [1,*]

1 Institute of Nuclear Physics, Polish Academy of Sciences, 31-342 Krakow, Poland; anna.wach@ifj.edu.pl (A.W.); rafal.fanselow@ifj.edu.pl (R.F.)
2 Physikalisch-Technische Bundesanstalt, Abbestr. 2-12, 10587 Berlin, Germany; yves.kayser@ptb.de
3 European XFEL GmbH, 22869 Schenefeld, Germany; christopher.milne@xfel.eu
4 Department of Chemistry, Uppsala University, 75120 Uppsala, Sweden; jacinto.sa@kemi.uu.se
* Correspondence: wojciech.blachucki@ifj.edu.pl (W.B.); jakub.szlachetko@ifj.edu.pl (J.S.)

Featured Application: In the present work, RXES planes are reconstructed with high energy resolution from the experimental spectra of the X-ray radiation emitted from a sample and of incident X-ray pulses delivered by an XFEL operated in the raw SASE mode. The dependence of the reconstructed RXES planes' quality on the number of recorded XFEL shots is studied.

Abstract: Aqueous iron (III) oxide nanoparticles were irradiated with pure self-amplified spontaneous emission (SASE) X-ray free-electron laser (XFEL) pulses tuned to the energy around the Fe K-edge ionization threshold. For each XFEL shot, the incident X-ray pulse spectrum and Fe Kβ emission spectrum were measured synchronously with dedicated spectrometers and processed through a reconstruction algorithm allowing for the determination of Fe Kβ resonant X-ray emission spectroscopy (RXES) plane with high energy resolution. The influence of the number of X-ray shots employed in the experiment on the reconstructed data quality was evaluated, enabling the determination of thresholds for good data acquisition and experimental times essential for practical usage of scarce XFEL beam times.

Keywords: X-ray free-electron laser (XFEL), resonant X-ray emission spectroscopy (RXES) with self-amplified spontaneous emission (SASE) XFEL beam; reconstruction of RXES planes

Citation: Błachucki, W.; Kayser, Y.; Wach, A.; Fanselow, R.; Milne, C.; Sá, J.; Szlachetko, J. Resonant X-ray Emission Spectroscopy with a SASE Beam. *Appl. Sci.* **2021**, *11*, 8775. https://doi.org/10.3390/app11188775

Academic Editor: Ion Sandu

Received: 28 August 2021
Accepted: 18 September 2021
Published: 21 September 2021

1. Introduction

The unique combination of high-brilliance and ultra-short pulses delivered by X-ray free electron lasers (XFELs) has opened up new possibilities for studying complex phenomena in physics [1], chemistry [2,3], biology [4,5], material science [6], as well as many other disciplines. The modern XFEL sources generate tunable femtosecond X-ray pulses with energies of up to tens of millijoules at wavelengths down to the Ångström level, enabling time-resolved measurements of structural and electronic dynamics down to femtosecond time scales [7,8]. However, the typical mode of X-ray pulse generation at XFELs is based on the self-amplified spontaneous emission (SASE) process [9]. In this process, the initial shot noise in the electron beam current produces spontaneous emission of photons that is further amplified by mutual interaction with the electron bunch over the undulator length, up to the saturation power. The stochastic nature of the SASE process provides large uncertainties in time, space, intensity, and energy of the X-ray pulses generated on a shot-to-shot basis, limiting the application of X-ray spectroscopy methods to well-defined self-seeded or monochromatized XFEL beams only.

Over the past few years, many developments have been made to overcome these limitations and take full advantage of the random nature of the XFEL pulses. One recently introduced approach is based on the reconstruction methodology that allows following electronic transitions with a temporal resolution solely restricted to the incident pulse duration [10]. It has been shown that the combination of the stochastic nature of SASE pulses

with non-invasive diagnostics can be used to extend the scope of X-ray spectroscopies at XFELs to two-dimensional X-ray spectroscopy techniques, i.e., resonant X-ray emission spectroscopy (RXES). The crucial aspect of the presented methodology was bypassing the monochromator and thus avoiding the temporal broadening of XFEL pulses related to the extinction length of X-rays in the monochromator crystal. Moreover, the experiment was performed in a scanning-free mode of detection for both incidence and emission X-ray spectra, thus allowing fast acquisition of desired signals. The presented reconstruction algorithm allowed to obtain high energy-resolution RXES planes based on the measured spectral distributions of a collection of individual incident non-monochromatized SASE pulses and each corresponding X-ray emission spectroscopy (XES) signal emitted from the studied sample. The method thus enables to map simultaneously the unoccupied and the occupied electronic states of the scattering atom exposed to short and intense SASE XFEL pulses. The reconstruction concept was further expanded in the work of Cavaletto et al. [11], demonstrating the application of noisy XFEL pulses to stimulated X-ray Raman experiments. Studies were focused on a model system with a conical intersection to illustrate resulting resolutions in time and spectral domains. Further, it has been demonstrated that narrow and chemically rich information in core-to-valence transitions of the pre-edge region at the Fe K edge has been obtained with our methodology [12].

In the present work, we evaluated the influence of the number of XFEL shots recorded on the quality of the RXES planes reconstructed with the previously reported algorithm [10]. The presented analysis facilitates planning an RXES experiment under SASE conditions at XFELs.

2. Materials and Methods

The experiment was performed at the X-ray Pump–Probe (XPP) instrument (SLAC National Accelerator Laboratory, Menlo Park, CA, USA) [13] of the Linac Coherent Light Source (LCLS) [14]. Four percent wt. aqueous solution of iron (III) oxide nanoparticles circulated in the form of a 200 µm-thick jet was irradiated with 35 fs-short (FWHM) pulses of 1.29×10^{12} photons at the repetition rate of 120 Hz. The beam spot on the sample had an area of 500 μm^2. The nanoparticles' average size was 30 nm and polypropylene glycol agent was added to the solution to prevent foaming. The mean photon energy was varied around the Fe K-edge ionization threshold (7123 eV) by ramping the electron beam energy up and down at the frequency of 5 Hz.

The spectrum of each incident SASE pulse was measured non-invasively with high energy resolution using a transmissive spectrometer [15] equipped with a thin bent Si(400) crystal and an ORCA detector composed of 2048×2048 square pixels with a side length of 6.5 µm. The spectrometer was adjusted to cover the energy range from 7090 to 7170 eV, which was broad enough to catch the full spectral envelope of each XFEL pulse accounting also for the XFEL jitter, and was more than sufficient for the incident photon energy range in the RXES maps. The average energy bandwidth was 52 meV/pixel, which was sufficient to resolve single spikes in the SASE spectra. The Fe Kβ XES spectra were acquired by means of a von Hámos spectrometer [16] composed of a cylindrically bent InSb(444) crystal and a CSPAD-140k detector [17] equipped with a matrix of 388×370 pixels, each having the dimensions of 110×110 μm^2. The von Hámos spectrometer's average energy bandwidth was 0.5 eV/pixel, and the expected energy resolution was 0.7 eV.

The RXES planes reconstruction is based on a matrix formalism, where for the number of SASE pulses k, the set of the measured emission spectra $\boldsymbol{S}_{kn}$, with n denoting the number of points in a single emission spectrum, is described with the following matrix equation [10]:

$$\boldsymbol{S}_{kn} = \boldsymbol{J}_{km} \cdot \boldsymbol{R}_{mn}, \quad (1)$$

with the set of the incident pulses' spectra $\boldsymbol{J}_{km}$, where m is the number of points in a single incident spectrum ($k > m$). In the above equation, the matrix $\boldsymbol{R}_{mn}$ is the RXES plane, i.e., representation of emission probability for incident photon energy indexed with m and

for emission energy indexed with n. The matrices $\boldsymbol{S}$ and $\boldsymbol{J}$ are observables and the RXES plane $\boldsymbol{R}$ can be determined using the Moore–Penrose pseudoinverse matrix ${\boldsymbol{J}_{km}}^{+}$ [10]:

$$\boldsymbol{R}_{mn} = {\boldsymbol{J}_{km}}^{+} \cdot \boldsymbol{S}_{kn}. \tag{2}$$

3. Results and Discussion

The RXES planes were reconstructed by means of Equation (2) for different numbers k of the measured incident and emission X-ray spectra. The measured data and the Fe Kβ RXES planes reconstructed for four different numbers of pulses are shown in Figure 1. For the analysis, we considered 1200, 6000, 12,000, 24,000, and 60,000 incidence pulses that, at 120 Hz repetition rate, correspond to the total acquisition time of 10, 50, 100, 200, and 500 s, respectively. In Figure 1′s left column, the measured incident SASE pulses' spectra are plotted. As shown, the spectra jitter around the Fe K-edge binding energy, but the average over a greater number of pulses (red line) takes on a Gaussian shape. In the central column, the measured Fe Kβ XES spectra are presented. Because of the XFEL beam jitter, certain pulses contained mainly photons with energy smaller than the Fe K-edge binding energy, while others delivered some or many photons with energy above the ionization threshold. As a result, some incident SASE pulses did not induce any Fe Kβ emission, while others induced some or strong emission, hence the plots' ragged character. The gaps appearing periodically along the vertical axis (pulse ordering number) in the Fe Kβ XES column result from the variation of photon energy controlled with a Vernier element, periodically disabling the Fe Kβ emission [18]. In Figure 1′s right column, the reconstructed Fe Kβ XES planes are presented. The obtained RXES planes provide detailed information on the occupied and unoccupied electronic states in the sample. For the increasing number of the processed pulses, the reconstructed RXES plane becomes less grainy, showing the electronic structure with better precision.

To quantify the noisiness $n(k)$ of the reconstructed RXES planes $I_k(E_1, E_2)$ with the number of pulses k, incidence energy E_1, and emission energy E_2, the following steps were taken. First, a residual $r(k, E_1, E_2)$ of the reconstructed 3D RXES plane was calculated with the plane reconstructed for $k_{\max} = 60,000$ XFEL pulses taken as the reference plane:

$$r(k, E_1, E_2) = I_k(E_1, E_2) - I_{k_{\max}}(E_1, E_2). \tag{3}$$

Second, the absolute value of residual function was integrated over the entire incident, and emission energy ranges covered in the experiment, which yielded a single number for each residual function. Finally, the obtained numbers were divided by the reference plane's integral, providing a relative deviation of the reconstructed plane from the reference one:

$$n(k) = \frac{\int |r(k, E_1, E_2)| \mathrm{d}E_1 \mathrm{d}E_2}{\int I_{k_{\max}}(E_1, E_2) \mathrm{d}E_1 \mathrm{d}E_2}. \tag{4}$$

The reconstructed RXES planes were processed in the described way, and the result, i.e., an estimate of the RXES planes' noisiness as a function of the number of SASE pulses, is shown in Figure 2. As expected, the noisiness decreases monotonically for the increasing number of pulses processed in the reconstruction and converges well with a $\sim 1/\sqrt{k}$ function (in blue) representing the expected error dependence. The plotted data can be used in the determination of the number of XFEL pulses needed to obtain the demanded accuracy of the RXES planes' reconstruction. In the case studied in this work, at least a few thousand pulses are required to maintain the statistical significance below 10%. For the very low number of pulses required, one should reckon with the potential necessity of reducing the number of points in the incident spectra (through either binning or cutting out a part of the spectrum) to fulfill the vital reconstruction condition $k > m$.

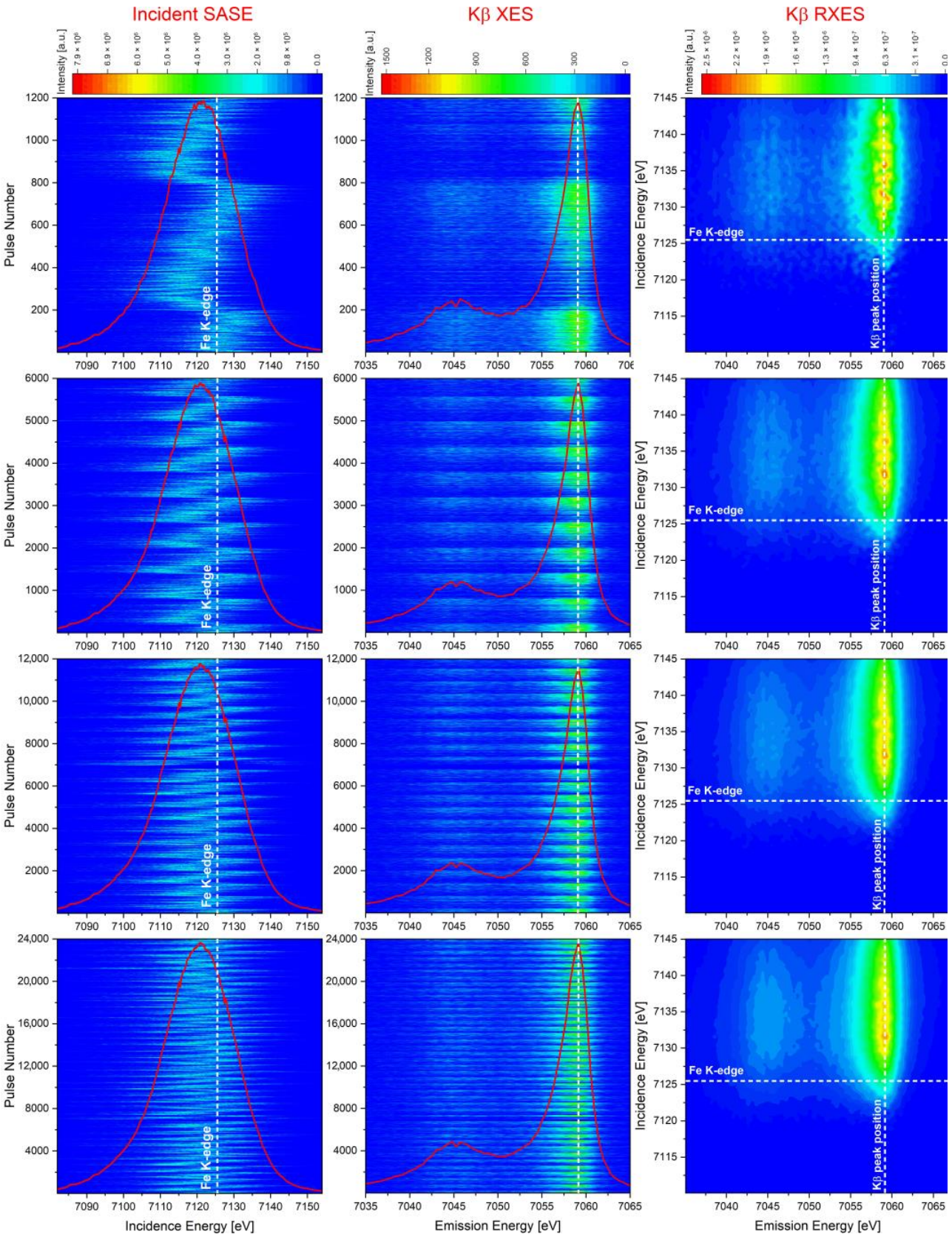

Figure 1. The measured incident SASE and Fe Kβ XES spectra (**left** and **central** column) and the Fe Kβ RXES planes (**right** column) reconstructed for: 1200, 6000, 12,000, and 24,000 pulses (rows 1–4).

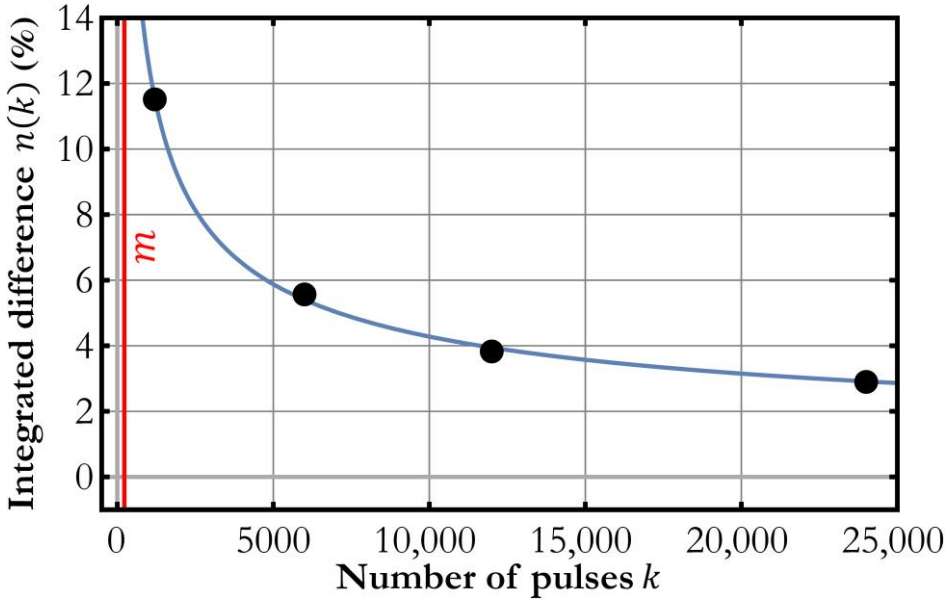

Figure 2. The dependence of the reconstructed 3D RXES plane's noisiness on the number of XFEL shots recorded (black) calculated with Equation (4) and estimation based on a function $\sim 1/\sqrt{k}$ (blue). Also shown is the methodological threshold m (red)—minimum number of shots required for reconstruction, equal to the number of points in the incident spectra (in the present study equal to 225).

4. Conclusions

In this work, we further investigated the possibility to perform simultaneous X-ray absorption spectroscopy (XAS) and X-ray emission spectroscopy (XES) measurement at XFELs with the stochastic SASE beam. The described methodology allows obtaining the combined XAS and XES data in the form of an RXES plane reconstructed from the measured incident SASE and X-ray emission spectra [10]. Conventional XAS spectrum or RXES plane acquisition involves special treatment of the incident X-ray beam, e.g., monochromatization [19], beam splitting [20], or seeding [21], which reduces the XFEL beam intensity on the sample or extends the XFEL pulse duration [22]. The described approach does not require any XFEL beam treatment and engages a scanning-free X-ray emission spectrometer, thus allowing a quick acquisition of the entire RXES plane at high energy resolution using the bright SASE beam and offering temporal resolution solely restricted to the pulse duration. The number of pulses required to reach the reconstructed RXES plane's precision of interest can be determined in a single measurement.

Author Contributions: Conceptualization, Y.K., J.S. (Jakub Szlachetko) and W.B.; methodology, Y.K. and W.B.; software, All authors; validation, J.S. (Jakub Szlachetko) and C.M.; formal analysis, W.B.; investigation, J.S. (Jakub Szlachetko) and W.B.; resources, All authors; data curation, W.B. and Y.K.; writing—original draft preparation, A.W., J.S. (Jakub Szlachetko) and W.B.; writing—review and editing, All authors; visualization, A.W., W.B. and J.S. (Jakub Szlachetko); supervision, All authors; project administration, J.S. (Jakub Szlachetko); funding acquisition, J.S. (Jakub Szlachetko). All authors have read and agreed to the published version of the manuscript.

Funding: This work was supported by the National Science Centre (Poland) under Grant No. 2017/27/B/ST2/01890 (for spectral and temporal properties of XFEL beams) and under Grant No. 2020/37/B/ST3/00555 (for electronic structure studies of nanoparticle systems).

Institutional Review Board Statement: Not applicable.

Informed Consent Statement: Not applicable.

Data Availability Statement: Raw data were generated at the X-ray Pump Probe instrument of the Linac Coherent Light Source. Derived data supporting the findings of the presented study are available from the corresponding authors on reasonable request.

Acknowledgments: Not applicable.

Conflicts of Interest: The authors declare no conflict of interest. The funders had no role in the design of the study; in the collection, analyses, or interpretation of data; in the writing of the manuscript, or in the decision to publish the results.

References

1. Rudek, B.; Son, S.-K.; Foucar, L.; Epp, S.; Erk, B.; Hartmann, R.; Adolph, M.; Andritschke, R.; Aquila, A.; Berrah, N.; et al. Ultra-efficient ionization of heavy atoms by intense X-ray free-electron laser pulses. *Nat. Photonics* **2012**, *6*, 858–865. [CrossRef]
2. Lemke, H.T.; Kjær, K.S.; Hartsock, R.; Van Driel, T.B.; Chollet, M.; Glownia, J.M.; Song, S.; Zhu, D.; Pace, E.; Matar, S.F.; et al. Coherent structural trapping through wave packet dispersion during photoinduced spin state switching. *Nat. Commun.* **2017**, *8*, 15342. [CrossRef] [PubMed]
3. Obara, Y.; Ito, H.; Ito, T.; Kurahashi, N.; Thürmer, S.; Tanaka, H.; Katayama, T.; Togashi, T.; Owada, S.; Yamamoto, Y.-I.; et al. Femtosecond time-resolved X-ray absorption spectroscopy of anatase TiO_2 nanoparticles using XFEL. *Struct. Dyn.* **2017**, *4*, 044033. [CrossRef] [PubMed]
4. Mara, M.W.; Hadt, R.G.; Reinhard, M.E.; Kroll, T.; Lim, H.; Hartsock, R.W.; Alonso-Mori, R.; Chollet, M.; Glownia, J.M.; Nelson, S.; et al. Metalloprotein entatic control of ligand-metal bonds quantified by ultrafast x-ray spectroscopy. *Science* **2017**, *356*, 1276–1280. [CrossRef] [PubMed]
5. Suga, M.; Akita, F.; Sugahara, M.; Kubo, F.A.M.; Nakajima, Y.; Nakane, T.; Yamashita, K.; Umena, Y.; Nakabayashi, M.; Yamane, T.; et al. Light-induced structural changes and the site of O=O bond formation in PSII caught by XFEL. *Nature* **2017**, *543*, 131–135. [CrossRef]
6. Mariette, C.; Lorenc, M.; Cailleau, H.; Collet, E.; Guérin, L.; Volte, A.; Trzop, E.; Bertoni, R.; Dong, X.; Lépine, B.; et al. Strain wave pathway to semiconductor-to-metal transition revealed by time-resolved X-ray powder diffraction. *Nat. Commun.* **2021**, *12*, 1239. [CrossRef] [PubMed]
7. Emma, P.; Bane, K.; Cornacchia, M.; Huang, Z.; Schlarb, H.; Stupakov, G.; Walz, D. Femtosecond and Subfemtosecond X-ray Pulses from a Self-Amplified Spontaneous-Emission–Based Free-Electron Laser. *Phys. Rev. Lett.* **2004**, *92*, 074801. [CrossRef]
8. Lindenberg, A.M.; Johnson, S.L.; Reis, D.A. Visualization of Atomic-Scale Motions in Materials via Femtosecond X-ray Scattering Technique. *Annu. Rev. Mater. Res.* **2017**, *47*, 425–449. [CrossRef]
9. Andruszkow, J.; Aune, B.; Ayvazyan, V.; Baboi, N.; Bakker, R.; Balakin, V.; Barni, D.; Bazhan, A.; Bernard, M.; Bosotti, A.; et al. First Observation of Self-Amplified Spontaneous Emission in a Free-Electron Laser at 109 nm Wavelength. *Phys. Rev. Lett.* **2000**, *85*, 3825–3829. [CrossRef]
10. Kayser, Y.; Milne, C.; Juranić, P.; Sala, L.; Czapla-Masztafiak, J.; Follath, R.; Kavčič, M.; Knopp, G.; Rehanek, J.; Błachucki, W.; et al. Core-level nonlinear spectroscopy triggered by stochastic X-ray pulses. *Nat. Commun.* **2019**, *10*, 476. [CrossRef]
11. Cavaletto, S.M.; Keefer, D.; Mukamel, S. High Temporal and Spectral Resolution of Stimulated X-ray Raman Signals with Stochastic Free-Electron-Laser Pulses. *Phys. Rev. X* **2021**, *11*, 011029.
12. Fuller, F.D.; Loukianov, A.; Takanashi, T.; You, D.; Li, Y.; Ueda, K.; Fransson, T.; Yabashi, M.; Katayama, T.; Weng, T.-C.; et al. Resonant X-ray emission spectroscopy from broadband stochastic pulses at an X-ray free electron laser. *Commun. Chem.* **2021**, *4*, 84. [CrossRef]
13. Chollet, M.; Alonso-Mori, R.; Cammarata, M.; Damiani, D.; Defever, J.; Delor, J.T.; Feng, Y.; Glownia, J.M.; Langton, J.B.; Nelson, S.; et al. The X-ray pump-probe instrument at the linac coherent light source. *J. Synchrotron Radiat.* **2015**, *22*, 503–507. [CrossRef] [PubMed]
14. Emma, P.; Akre, R.; Arthur, J.; Bionta, R.; Bostedt, C.; Bozek, J.; Brachmann, A.; Bucksbaum, P.; Coffee, R.; Decker, F.-J.; et al. First lasing and operation of an ångstrom-wavelength free-electron laser. *Nat. Photonics* **2010**, *4*, 641–647. [CrossRef]
15. Rich, D.; Zhu, D.; Turner, J.; Zhang, D.; Hill, B.; Feng, Y. The LCLS variable-energy hard X-ray single-shot spectrometer. *J. Synchrotron Radiat.* **2016**, *23*, 3–9. [CrossRef] [PubMed]
16. Szlachetko, J.; Nachtegaal, M.; De Boni, E.; Willimann, M.; Safonova, O.; Sa, J.; Smolentsev, G.; Van Bokhoven, J.A.; Dousse, J.-C.; Hoszowska, J.; et al. A von Hamos x-ray spectrometer based on a segmented-type diffraction crystal for single-shot x-ray emission spectroscopy and time-resolved resonant inelastic x-ray scattering studies. *Rev. Sci. Instrum.* **2012**, *83*, 103105. [CrossRef] [PubMed]
17. Blaj, G.; Caragiulo, P.; Carini, G.; Carron, S.; Dragone, A.; Freytag, D.; Haller, G.; Hart, P.; Hasi, J.; Herbst, R.; et al. X-ray detectors at the linac coherent light source. *J. Synchrotron Rad.* **2015**, *22*, 577–583. [CrossRef] [PubMed]
18. Winkelmann, L.; Choudhuri, A.; Chu, H.; Hartl, I.; Li, C.; Mohr, C.; Müller, J.; Peters, F.; Pfeiffer, S.; Salman, S.; et al. The European XFEL Photocathode Laser. In Proceedings of the 39th Free Electron Laser Conference, Hamburg, Germany, 26–30 August 2019; JACoW Publishing: Geneva, Switzerland, 2019; Volume 39, pp. 423–426.

19. Lemke, H.T.; Bressler, C.; Chen, L.X.; Fritz, D.M.; Gaffney, K.J.; Galler, A.; Gawelda, W.; Haldrup, K.; Hartsock, R.W.; Ihee, H.; et al. Femtosecond X-ray Absorption Spectroscopy at a Hard Xray free electron laser: Application to spin crossover dynamics. *J. Phys. Chem. A* **2013**, *117*, 735–740. [CrossRef]
20. Katayama, T.; Inubushi, Y.; Obara, Y.; Sato, T.; Togashi, T.; Tono, K.; Hatsui, T.; Kameshima, T.; Bhattacharya, A.; Ogi, Y.; et al. Femtosecond x-ray absorption spectroscopy with hard xray free electron laser. *Appl. Phys. Lett.* **2013**, *13*, 131105. [CrossRef]
21. Kroll, T.; Kern, J.; Kubin, M.; Ratner, D.; Gul, S.; Fuller, F.D.; Löchel, H.; Krzywinski, J.; Lutman, A.; Ding, Y.; et al. X-ray absorption spectroscopy using a self-seeded soft X-ray free-electron laser. *Opt. Express* **2016**, *24*, 22469–22480. [CrossRef]
22. Shastri, S.D.; Zambianchi, P.; Mills, D.M. Dynamical diffraction of ultrashort X-ray free-electron laser pulses. *J. Synchrotron Radiat.* **2001**, *8*, 1131–1135. [CrossRef]